

## Contents

<a href="#">1 Article Information</a>	1
<a href="#">2 Motivation and Problem Addressed</a>	1
<a href="#">3 DFT Calculations and Thermochemistry Modeling</a>	2
<a href="#">4 Highlights of Results</a>	4
<a href="#">5 Critical Review</a>	5

## 1 Article Information

The article reviewed in this report is the following:

Zhang, B., Duan, Y., Johnson, K. *Density functional theory study of CO<sub>2</sub> capture with transition metal oxides and hydroxides*. (2012) **The Journal of Chemical Physics**, 136(6):064516.

This report is organized as follows. Section [2](#) motivates and defines the objectives of the problem addressed in the article. Section [3](#) summarizes the authors' approach to performing DFT calculations and modeling the thermochemistry of the CO<sub>2</sub> capture. Section [4](#) highlights some of the results obtained. Finally, section [5](#) presents a critical review of the methodology and results.

## 2 Motivation and Problem Addressed

Carbon dioxide (CO<sub>2</sub>) is one of the primary greenhouse gases. Therefore, researchers have investigated efficient ways to capture and sequester CO<sub>2</sub> in order to mitigate its effect on global climate change. There are three classes of CO<sub>2</sub> capture technologies:

- **Pre-combustion:** Removal of CO<sub>2</sub> from the fossil fuel prior to combustion
- **Post-combustion:** CO<sub>2</sub> capture from the flue gas after combustion of the fossil fuel (traditionally scrubbing with liquid monoethanolamine (MEA))
- **Oxy-fuel:** Combustion of fossil fuel with pure oxygen rather than air (avoids NO<sub>x</sub> and concentrates CO<sub>2</sub>)

The main objectives of the article are as follows:

- Investigate the efficiency of solid sorbents to capture CO<sub>2</sub>;
- Compute phase diagrams of reactions between sorbents and CO<sub>2</sub>;

- Assess the accuracy of five different Density Functional Theory (DFT) generalized gradient functionals for the prediction of the reaction thermodynamics of various transition metal oxides and hydroxides;
- Screen these materials for suitability in pre-combustion and post-combustion CO<sub>2</sub> capture.

### 3 DFT Calculations and Thermochemistry Modeling

Two computational packages were employed to perform the DFT calculations: VASP and GPAW. Functionals were used to calculate the ground state energies of all the solid phase and gas phase compounds. Table 1 gives the details of the features used in each package. The  $k$ -point meshes generated for both packages were generated with a spacing of around  $0.027 \text{ \AA}^{-1}$  between  $k$ -points along the axes of the reciprocal unit cells.

Table 1: Features of each computational package.

Feature	VASP	GPAW
CE Interactions	PAW potentials	—
XC Potentials	PW91 (CG), PBEsol (QN)	PBE, TPSS, revTPSS
Energy convergence	0.01 meV	$10^{-6}$ eV/atom, grid spacing of $0.15 \text{ \AA}$
Energy cut-off	520 eV	520 eV
$k$ -point meshes	Monkhorst-Pack	Monkhorst-Pack

where CE stands for core-electron, XC stands for exchange-correlation, PAW stands for Projector Augmented-Wave, CG stands for conjugate-gradient method, QN stands for quasi-Newton method.

The thermochemistry for the CO<sub>2</sub> capture reactions was modeled using statistical mechanics ideal gas expressions. The temperature-related free energy of gas species is given by:

$$G^0 = U + PV - TS \approx U_{\text{DFT}} + U_{\text{ZPE}} + U_{\text{trans+rot}}(T) + U_{\text{vib}}(T) + PV - TS(T) \quad (1)$$

where  $U_{\text{DFT}}$  is the electronic total energy of the material as computed using DFT,  $U_{\text{ZPE}}$  is the zero point energy (ZPE) of the gas, and

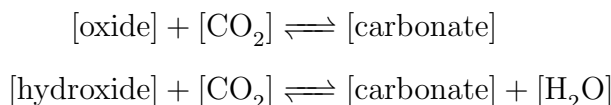
$$U_{\text{trans+rot}}(T) = \begin{cases} \frac{5}{2}RT & \text{for linear molecules} \\ \frac{6}{2}RT & \text{for nonlinear molecules} \end{cases}$$

$$U_{\text{vib}}(T) = \sum_i \frac{R\theta_i}{\exp(\theta_i/T) - 1}$$

$$S(T) = A \ln(t) + Bt + \frac{Ct^2}{2} + \frac{Dt^3}{3} - \frac{E}{2t^2} + F$$

where  $t = T/1000$  and parameters ( $A$ ,  $B$ ,  $C$ ,  $D$ ,  $E$ ,  $F$ ) are taken from NIST chemistry webbook (Shomate Equation).

The reactions are expressed in the following general way:



Thus, the free energy change of reaction is calculated by:

$$\Delta G = \Delta G_{\text{solid}} + \Delta G_{\text{CO}_2} \quad (2)$$

or

$$\Delta G = \Delta G_{\text{solid}} + \Delta G_{\text{CO}_2} - \Delta G_{\text{H}_2\text{O}} \quad (3)$$

for reactions without and with water, respectively.

Since the volume change due to gas generation is very large relative to the volume change of solid materials, we can neglect the volume change of solid phases without significant loss of accuracy. If the activities of all solid components are taken to be 1, the equilibrium pressure of the overall reaction can then be written as:

$$\frac{P_{\text{CO}_2}}{P_0} = \exp\left(-\frac{\Delta G}{RT}\right) \quad (4)$$

where  $P_0$  is the standard state pressure (1 bar), or

$$\frac{P_{\text{CO}_2}}{P_{\text{H}_2\text{O}}} = \exp\left(-\frac{\Delta G}{RT}\right) \quad (5)$$

for reactions without and with  $\text{H}_2\text{O}$ , respectively. The van't Hoff plots are obtained by plotting the equilibrium pressures from equations (4) or (5) as a function of the inverse absolute temperature.

Phase diagrams for the solids were obtained by minimizing the grand-canonical Gibbs free energy of a system where all possible solid phases are in contact with a gas-phase reservoir having specified partial pressures of  $\text{CO}_2$  and  $\text{H}_2\text{O}$ . Hence, the optimization problem solved is to minimize

$$G(T, \mu_{\text{gas}}) = \sum_{j=1}^S x^j F^j(T) - \sum_k \sum_{j=1}^S \mu_k^{\text{gas}}(T, p) x_k^{j, \text{gas}} \quad (6)$$

subject to (mass conservation constraint):

$$\sum_{i=\text{metal}}^M f_i = \sum_{i=\text{metal}}^M \sum_{j=1}^S x^{j, \text{solid}} b_i^{j, \text{solid}} = 1 \quad (7)$$

where  $F^j(T)$  is the free energy of solid phase  $j$  (ignoring the  $pV$  term contribution),  $S$  is the number of solid substances,  $\mu_k^{\text{gas}}(T, p)$  is the chemical potential of gas species  $k$  ( $\text{CO}_2$  and  $\text{H}_2\text{O}$ ),  $x^j$  is the unknown mole fraction of phase  $j$  coexisting at a given composition, temperature, and pressure,  $x_k^{j, \text{gas}}$  is the theoretical mole fraction of gas species  $k$  contained

in phase  $j$ ,  $f_i$  is the molar ratio of solid element  $i$  in all solids,  $b_i^{j,\text{solid}}$  represents the number of atoms of type  $i$  in one formula unit of phase  $j$ , and  $M$  is the number of elements.

The authors chose sufficiently small intervals of temperature and pressure to ensure adequately small chemical potential changes between two steps in order to guarantee single step reactions.

## 4 Highlights of Results

Figure 1 shows partial results for the DFT calculations. It can be noted that better agreement with experimental values of lattice parameters were obtained when using PBEsol for compounds containing Zn and Cd except  $\text{Zn}(\text{OH})_2$  and using PW91 for compounds containing Mn and Ni. Regarding entropies calculated from frozen-phonon approach, discrepancies are within 10 J/(mol K) except for NiO and  $\text{Ni}(\text{OH})_2$ .

Compound	Space group	Lattice parameters <sup>a</sup>			Enthalpy of formation <sup>b</sup> (kJ/mol)			Entropy <sup>c</sup> (J/mol K)	
		Expt.	PW91	PBEsol	Expt.	PW91	PBEsol	Expt.	PW91
MnO	$Fm\bar{3}m$	a = 4.446	a = 4.3281	a = 4.3367	− 385.2	− 246.1	− 231.4	59.71	49.98
NiO	$Fm\bar{3}m$	a = 4.1944	a = 4.1809	a = 4.1056	− 239.7	− 103.7	− 108.2	37.99	53.75
ZnO	$P6_3mc$	a = 3.2525	a = 3.2806	a = 3.2389	− 350.5	− 289.7	− 288.4	43.64	45.31
		c = 5.2111	c = 5.2978	c = 5.2276					
		$\gamma = 120$	$\gamma = 120$	$\gamma = 120$					
CdO	$Fm\bar{3}m$	a = 4.6948	a = 4.7758	a = 4.7083	− 258.4	− 207.8	− 211.4	54.81	60.21
$\text{Mn}(\text{OH})_2$	$P\bar{3}m1$	a = 3.322	a = 3.3496	a = 3.2991	− 695.4	− 529.2	− 522.7	99.2	86.15
		c = 4.734	c = 4.7417	c = 4.5419					
		$\gamma = 120$	$\gamma = 120$	$\gamma = 120$					
$\text{Ni}(\text{OH})_2$	$P\bar{3}m1$	a = 3.13	a = 3.1665	a = 3.1203	− 529.7	− 381.9	− 397.8	88.0	70.42
		c = 4.63	c = 4.5814	c = 4.3581					
		$\gamma = 120$	$\gamma = 120$	$\gamma = 120$					
$\text{Zn}(\text{OH})_2$	$P\bar{3}m1$	a = 3.194	a = 3.2389	a = 3.1901	− 641.9	− 540.6	− 561.3	81.2	82.59
		c = 4.714	c = 4.6598	c = 4.4824					
		$\gamma = 120$	$\gamma = 120$	$\gamma = 120$					
$\text{Cd}(\text{OH})_2$	$I1m1$	a = 5.688	a = 5.7868	a = 5.6959	− 560.7	− 497.4	− 513.6	96.0	93.45
		b = 10.28	b = 10.2725	b = 10.0532					
		c = 3.42	c = 3.4943	c = 3.4321					
		$\beta = 91.4$	$\beta = 88.889$	$\beta = 88.548$					

Figure 1: Partial results of DFT calculations.

Figure 2 shows results for the thermochemistry calculations. HSC CHEMISTRY is a chemical reaction and equilibrium software package that can be used to calculate reaction equilibrium based on correlation of experimental data. Relatively large differences were observed between the calculated enthalpies of reaction at 298.15 K from all DFT methods and the experimentally measured values. PBEsol functional performs much better on average. Reaction entropies lie in between the HSC values (in the parenthesis) and the experimental data for the Mn-containing reactions.

Reaction	$\Delta H^0$ Expt. <sup>a</sup>	$\Delta H_{\text{PW91}}$	$\Delta H_{\text{PBE}}$	$\Delta H_{\text{PBEsol}}$	$\Delta H_{\text{TPSS}}$	$\Delta H_{\text{revTPSS}}$	$\Delta H$ HSC <sup>c</sup>	$\Delta S^0$ Expt. <sup>d</sup>	$\Delta S$ Calc. <sup>e</sup>
MnO + CO <sub>2</sub> $\rightleftharpoons$ MnCO <sub>3</sub>	-115.4	-77.71	-70.27	-100.85	-95.35	-117.65	-102.77	-187.71 (-167.83)	-176.29
NiO + CO <sub>2</sub> $\rightleftharpoons$ NiCO <sub>3</sub>	-70.18	-52.57	-65.89	-81.27	-112.80	-141.90	-63.05	-166.39	-194.78
ZnO + CO <sub>2</sub> $\rightleftharpoons$ ZnCO <sub>3</sub>	-68.8	-29.63	-36.33	-67.83	-108.59	-147.30	-68.76	-175.04	-174.01
CdO + CO <sub>2</sub> $\rightleftharpoons$ CdCO <sub>3</sub>	-98.73	-81.50	-78.91	-105.47	-117.64	-138.89	-99.36	-176.11	-173.77
Mn(OH) <sub>2</sub> + CO <sub>2</sub> $\rightleftharpoons$ MnCO <sub>3</sub> + H <sub>2</sub> O	-47.0	-21.74	-16.98	-45.57	-55.70	-75.52	-33.88	-38.4 (-18.53)	-23.41
Ni(OH) <sub>2</sub> + CO <sub>2</sub> $\rightleftharpoons$ NiCO <sub>3</sub> + H <sub>2</sub> O	-21.98	-1.53	-22.26	-27.72	-91.57	-121.63	-14.92	-27.6	-22.40
Zn(OH) <sub>2</sub> + CO <sub>2</sub> $\rightleftharpoons$ ZnCO <sub>3</sub> + H <sub>2</sub> O	-19.2	-5.96	-17.88	-30.98	-90.23	-121.25	-19.18	-23.8	-22.24
Cd(OH) <sub>2</sub> + CO <sub>2</sub> $\rightleftharpoons$ CdCO <sub>3</sub> + H <sub>2</sub> O	-38.2	-19.11	-11.29	-39.36	-50.29	-64.39	-38.69	-28.5	-17.97

<sup>a</sup>All the experimental values are computed from data in Table I at 298.15 K.

<sup>b</sup>Enthalpies calculated with different functionals at 298.15 K including finite temperature phonon contributions.

<sup>c</sup>Values taken from HSC database, at 303.15 K.

<sup>d</sup>Experimental values are computed from data in Table I, at 298.15 K; values in the parenthesis are taken from HSC database at 303.15 K.

<sup>e</sup>Calculated with the PW91 functional via the frozen-phonon method at 300 K.

Figure 2: Results of thermochemistry calculations.

## 5 Critical Review

The following conclusions can be made:

- Choice of exchange-correlation functionals directly affect the accuracy of DFT calculations
- LDA usually underestimates lattice constants for solids, whereas GGA usually overestimates them
  - Lattice constants play an important role in determining a number of properties
- “Higher-level” functionals (TPSS and revTPSS) performed better than GGA at predicting the enthalpy of formation of carbonates and oxides
  - Reaction enthalpies computed with these meta-GGA functionals are not as accurate as data computed from the PBEsol functional
  - May be due to the use of pseudopotentials that are not tuned for meta-GGA functionals
- Screening of metals for CO<sub>2</sub> capture
  - All the oxides may be useful for post-combustion CO<sub>2</sub> capture
  - Only MnO and CdO are possibilities for pre-combustion capture
  - None of the hydroxides are suitable for CO<sub>2</sub> capture (they decompose)

From section 3, it is clear that one approximation used in the modeling is the ideal gas law. Even though the authors listed the convergence criteria in terms of energy, they did not report if multiple DFT calculations were performed for different values of the energy cutoff in order to check for convergence. In order to be able to reproduce the calculations, I would need access to the Inorganic Crystal Structure Database (ICSD). Finally, the authors did not explicitly state the values for the parameters in the DFT packages, which could be a source of discrepancies when trying to reproduce the results.